Complex Weldment Properties: Trends in Predictive Power

H. K. D. H. Bhadeshia
University of Cambridge

Proceedings of the 6th International Conference on *Trends in Welding Research*, ASM International, Atlanta, Georgia, USA, 2002.

Abstract

We are entering an era where it may become possible to calculate important mechanical properties such as toughness and fatigue. Attempts to do this for weldments have opened up new avenues of research, aspects of which are described here. A recommendation is made about the optimum scheme for modelling materials failure.

Introduction

Our theoretical understanding of the various aspects of welding varies in the solidity of its foundations and in its predictive powers [1]. Many calculations involved are very difficult. The most intractable of these problems lies in *predicting* the mechanical behaviour of a weldment [2,3]. For there are many variables, including a variety of heterogeneities, the mean chemical composition, processing parameters, heat treatments, imperfections, and changes that occur during service, which determine performance.

> Mechanical properties can be measured with precision and the data used in safe design. But given a comprehensive description of material and process parameters, it is not yet possible to predict most of these properties.

There are many properties of interest. But to illustrate the difficulties and the way forward, I shall describe just two, the hardness and the toughness.

Hardness

It is common practice to design the welding procedure and the heat treatment to keep the hardness below some critical value based on experience. The hardness is often a measure of the potential for brittle fracture or the susceptibility to hydrogen–induced or stress–corrosion cracking [4]. This, of course, is the reason for the existence of carbon–equivalent equations where hardenability is kept below some maximum value in order to avoid unacceptable peak values in the heat–affected zones (HAZ's) of welds. A typical plot of how the hardness is expected to vary in the HAZ of a quenched and tempered martensitic steel is illustrated in Fig. 1 [5].

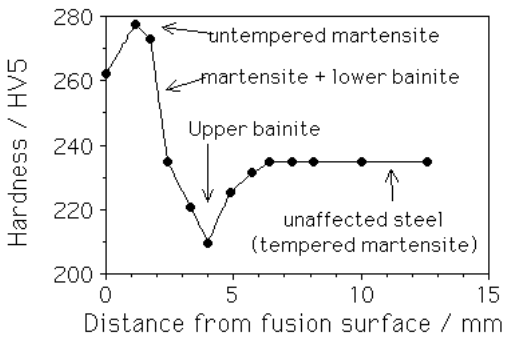

Fig. 1: Typical variation in hardness in the heat affected zone of QT steel [5].

The detailed variation in HAZ hardness, of the kind illustrated in Fig. 1, is due to a combination of factors including the gradients in the austenite grain structure, the variation in the thermal cycle experienced as a function of position and the chemical composition of the steel itself. The complex transformations in the HAZ were modelled by Ion, Easterling and Ashby in 1984 [6]. The model contained a distributed heat source to represent the welding arc, adapted from

Rosenthal's theory of heat flow. A key feature of the model was the concept of kinetic strength, a parameter which, by combining time and temperature, enables the effect of continuous heating or continuous cooling on the kinetics of transformations to be modelled. They were therefore able to calculate the dissolution and growth rates of carbides and nitrides during the heating part of the thermal cycle, and hence the effect of microalloying elements on the growth of austenite grains in the heat affected zone. Transformations during cooling were modelled using a representation of experimental continuous cooling transformation diagrams within a loose Avrami formulation. Finally, the hardness was related to the microstructure using a rule of mixtures, the hardnesses of the individual phases being estimated from empirical equations containing chemical composition and cooling rate as variables. With appropriate calibration, Ion *et al.* demonstrated a model which not only gave reasonable fit with experimental data, but also permitted all the trends to be reproduced in an self–consistent manner which could be represented on 'HAZ maps'.

Similar work on the hardness of hot–wire laser welds has been reported by Metzbower *et al.* [7], on the basis of calculated fusion–zone microstructure [8].

Hardness of the fusion zone: The development of microstructure is influenced by the chemical driving force, a variety of rate phenomena and spatial interference between growing particles. The microstructure of the fusion zone of a weld has been modelled using such a framework of thermodynamics, individual–particle kinetics and overall transformation kinetics [8,9,10]. It is possible to obtain quite reasonable estimates of weld metal microstructures as a function of the detailed chemical composition, welding conditions and other relevant parameters. Some example calculations are illustrated in Fig. 2, which shows the dramatic effects of carbon and boron on the microstructure [9].

For an individual phase, the strength can be factorised into a number of intrinsic components [2]:

$$\sigma = \sigma_{Fe} + \sum_i x_i \sigma_{SS_i} + x_C \sigma_C + K_L\{L\} + K_D \rho_D^{0.5}$$

where x_i is the concentration of a substitutional solute which is represented here by a subscript i. The other terms in this equation can be listed as follows:

K_L strengthening due to 'grain' size, $115\,\mathrm{MN\,m^{-1}}$
K_D dislocation strengthening, $7.34 \times 10^{-6}\,\mathrm{MN\,m^{-1}}$
σ_{Fe} pure, annealed Fe, $219\,\mathrm{MN\,m^{-2}}$ at 300 K
σ_{SS_i} substitutional solute (i) strengthening
σ_C solid solution strengthening due to carbon
ρ_D dislocation density, typically $10^{16}\,\mathrm{m^{-2}}$
$\overline{L}$ measure of the ferrite plate size, typically 0.2μm

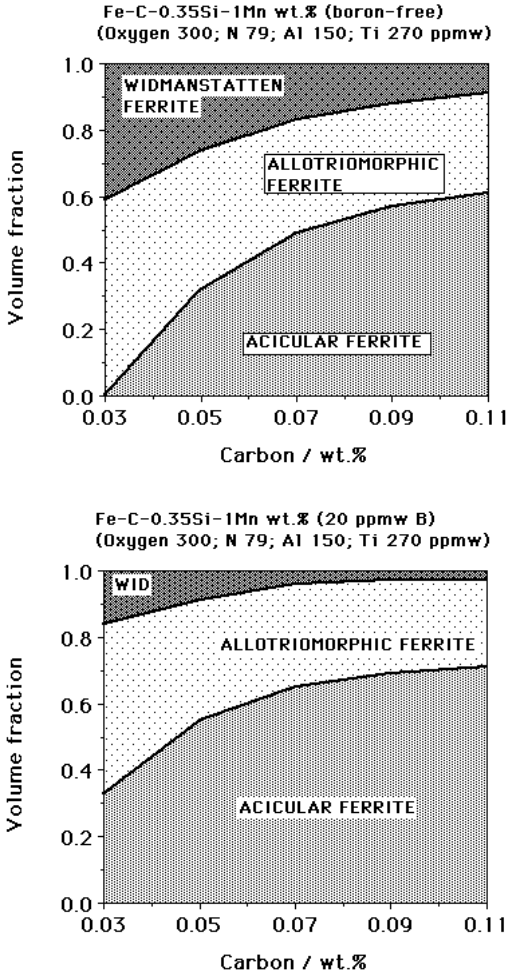

Fig. 2: Calculated microstructures of manual metal arc weld deposits as a function of chemical composition. The boron concentration makes a remarkable difference to the microstructure.

Given the microstructure, the yield strength can be estimated from that of the individual phases, either as a rule of mixtures [2], *i.e.* $\sigma = \sum_i \sigma_i V_i$ where V_i is the fraction of phase i, and σ_i the corresponding strength. Alternatively, a more sophisticated composite strengthening theory may be used [11,12]. A rule of mixtures will work well when each of the phases has a substantial presence in the microstructure; it would not be appropriate to apply it to a small fraction of precipitate present in a matrix. It can be shown that the rule fails when there are large differences in the mechanical properties of the constituent phases, as illustrated in Fig. 3(i). Fig. 2 shows that the microstructure can be particularly sensitive to carbon at low concentrations; Fig. 3(ii) shows that this is

reflected in the calculated strength. The calculated strength can be converted into hardness.

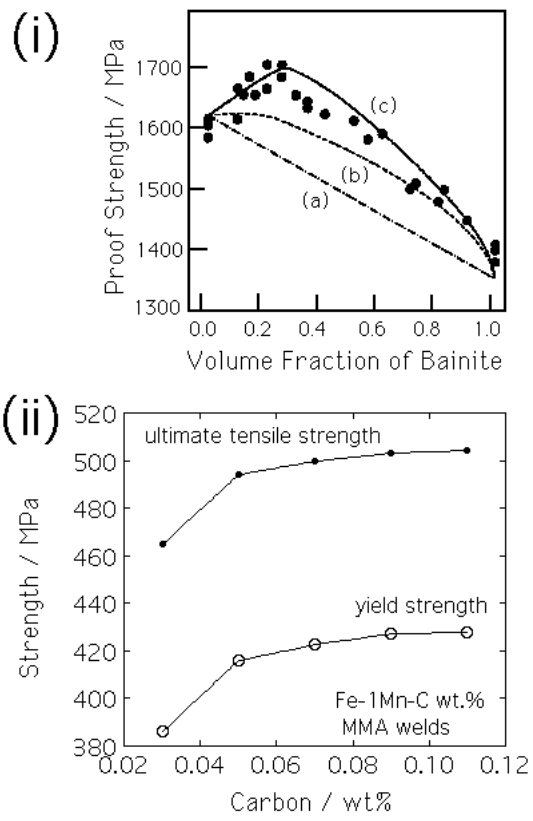

Fig. 3: (i) Strength of mixtures of bainite and martensite. Curve (a) shows the strength calculated using the rule of mixtures, (b) the strength including constraint but neglecting the detailed chemical composition of the individual phases and (c) the model including constraint and composition [14]. The points are experimental data from [15]. (ii) Calculated yield and ultimate tensile strength of weld metal as a function of the carbon concentration [2]

Hardness changes due to tempering: Apart from the heat–affected zone, many welding alloys, including those used in the construction of submarines and power plant, have a martensitic microstructure. It is useful then to be able to estimate hardness changes during heat treatment. Tempering martensite leads to the precipitation of carbon from solid solution, followed by recovery and recrystallisation. All of these processes involve some combination of nucleation, growth and overall kinetics. There is an impressive model due to Venugopalan and Kirkaldy which partly addresses these issues [16]. It is not appropriate to present here the full theory, but some equations are discussed in order to illustrate the level of sophistication. For example, account is taken of both lattice diffusion (D_L) and dislocation pipe diffusion (D_P) so the effective diffusion coefficient is

$$D_{eff} = D_L(1-f) + D_P f$$

where f is the fraction of atoms at the dislocation pipes. In this way, it is also possible to account for the dislocation cells (size L) that exist in martensitic microstructures. Indeed, the dislocation cells are allowed to coarsen alongside the precipitate dispersion using pinning and kinetic theory:

$$\frac{d(L^2)}{dt} = \left(1 - \frac{L}{L_l}\right) k_0 \exp\left\{-\frac{Q}{RT}\right\}$$

where k_0 and Q are kinetic constants and $L_l = 8r^*/3V_V$ is the limiting grain size given by standard pinning theory, V_V is the volume fraction of precipitates and r^* the mean precipitate size. The variation in r^* is modelled using Ostwald ripening theory adapted for multicomponent diffusion, which is dealt with quite rigourously in a consistent thermodynamic framework. The model requires an input of the initial cementite size, which the authors represent using an empirical equation based on experimental data for a large number of steels. Once the microstructure is calculated in this way, dislocation theory is used to estimate the yield strength and hence the hardness. The agreement between experiment and theory is found to be very good for a large number of alloys, both in terms of microstructure and strength.

In spite of its success, the theory cannot handle complications such as transitions between carbides. Although the theory for complex precipitation reactions is now available [17], there is no corresponding link between the calculated microstructure and the hardness. A different approach could be based on Avrami theory in which the extent ξ of the reaction can be assumed to be related to a normalised change in the hardness as follows:

$$\begin{aligned} \xi\{t\} =& 1 - \exp\{-k_A t^n\} \\ & \text{with} \qquad \xi\{t\} = \frac{H_0 - H\{t\}}{H_0 - H_F} \\ & \text{and} \qquad k_A = k_0 \exp\left\{-\frac{Q}{kT}\right\} \end{aligned} \tag{1}$$

where T is the absolute temperature, t is the time in hours, and k_0, Q and n are rate constants, H_0 is the hardness of untempered martensite, H_F is the hardness in the fully softened condition and $H\{t\}$ the hardness after an isothermal heat treatment.

Although the relationship in equation 1 has some justification in science, it nevertheless is a simplification of the real processes that happen during tempering. Discovery of the rate constants by fitting

to experimental data nevertheless provides a convenient method of interpolating and extrapolating the data. The method also suggests that in deriving the empirical fitting–parameters, the variables of interest are not T, t and ξ, but rather T^{-1} and $\ln\{t\}$ with $\ln\{-\ln\{1-\xi\}\}$. The results from an analysis of this kind are illustrated in Fig. 4.

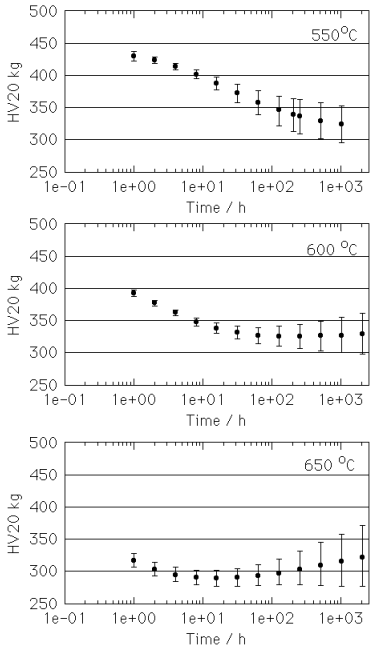

Fig. 4: The calculated hardness for Fe 0.21C 0.41Si 0.33Mn 1.77Cr 0.41Mo 3.87Ni wt% steel, with a martensitic microstructure, as a function of the tempering temperature and time [18]

Some experimental data for the steel described in Fig. 4 are reproduced in Fig. 5 in order to reveal complications, not accounted for in the theories described, when conducting post–weld heat treatments. Such heat treatments have the intention of reducing the hardness, but it is sometimes forgotten that the temperature at which austenite formation begins can be quite low for many modern alloys which contain relatively large concentrations of solutes. Thus, the hardness following tempering at 750 °C is greater than for the 650 °C samples. This is because the $Ae1$ temperature of the steel has been exceeded so that austenite forms during post–weld heat treatment; its subsequent transformation into untempered martensite is the reason for the increase in hardness. Effects like these have been reported previously in the context of welding alloys [19].

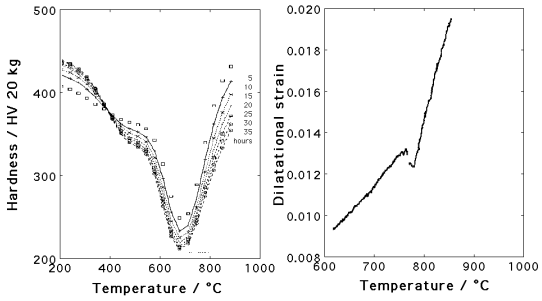

Fig. 5: (a) The hardness of the $3\frac{1}{2}$Ni alloy as a function of tempering temperature and time, illustrating the consequence of austenite formation at temperatures beyond $Ae1$. (b) Dilatometer experiment showing that during continuous heating transformation at $2^{\circ}\mathrm{C\,s}^{-1}$, showing the beginnings of austenite formation at about 740°C. [18]

There are useful ways of expressing hardness and limited models relating structure to hardness. It is evident, however, that there is no method for predicting the hardness in general.

Scatter & Information Theory

It is well known that there is scatter in measurements of fracture toughness of wrought and welded steels. Some of the scatter has its origins in the nonuniform microstructure typical of welds. A quantitative measure of such heterogeneity is the so–called microstructural entropy [20–22]. If X is a random variable assuming the value i with probability p_i, $i = 1, \ldots, n$, the entropy of X, as a logarithmic measure of the mean probability, is

$$H\{X\} = -\sum p_i \ln\{p_i\}.$$

$H\{X\}$ is zero for $p_i = 1$, and has a maximum value $\ln\{n\}$ when $p_1 = \ldots = p_n = \frac{1}{n}$.
For a typical weld microstructure, it follows that

$$H = -[V_\alpha \ln\{V_\alpha\} + V_a \ln\{V_a\} + V_w \ln\{V_w\}]$$

where V_α, V_a and V_w are the volume fractions of allotriomorphic, acicular and Widmanstätten ferrite respectively. H has been found to correlate well against the observed scatter in Charpy–toughness data [11], and hence can be used in the design of reliable microstructures (Fig. 6).

The term "local brittle zone" (LBZ), coined by Fairchild [23] is another cause of scatter. An LBZ is

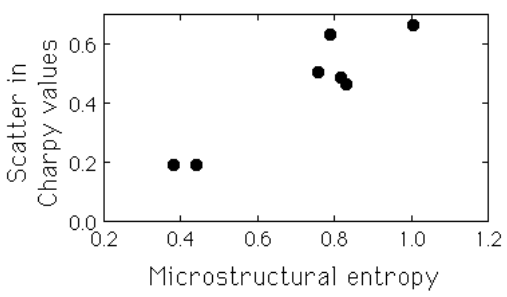

Fig. 6: A measure of the scatter in Charpy values, versus a measure of the heterogeneity of microstructure. A uniform microstructure has a small value of entropy H.

a small region of hard phase (usually martensite) in the heat–affected zone of a weld. A toughness test will record a low value if it samples the zone, but a high value if it does not. It has been claimed that the lower bound toughness values decrease as the fraction of the hard phase in the form of LBZ's increases [24, but the data in fact reveal a minimum in toughness with increasing martensite content [25]. This is because not all LBZ's are brittle, only those in which the martensite contains a large carbon concentration. When austenite transforms to ferrite at high temperatures it becomes enriched with carbon. The extent of enrichment depends on the fraction of ferrite; a large fraction is needed for the remaining austenite to transform into high carbon martensite LBZ's. Indeed, it has been demonstrated that the zones of martensite are not problematic in high hardenability steels where the amount of ferrite is small; the corresponding large fraction of relatively low–carbon martensite cannot be regarded as a local brittle zone.

The formation of LBZ's can be expressed quantitatively [26], as a function of cooling conditions, austenite grain structure and alloy chemistry. The condition favouring the existence of LBZ's was taken to be that 90% of the austenite should transform before the onset of martensitic transformation. The theory predicts correctly that LBZ's are more likely in regions which experience multiple thermal cycles within the austenite formation range; that they should form more readily when the austenite grain size is small; and that an increase in hardenability produces martensite zones which are not brittle (Fig. 7).

There is an understanding of scatter, but it is a loose understanding. Wouldn't it be nice to embody scatter in all aspects of weld modelling? After all, it is present without exception in all welds.

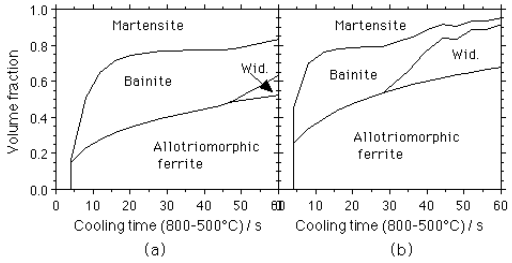

Fig. 7: A large amount of transformation prior to martensite a local zone more brittle. Hence, the Fe-0.1C-1Mn wt.% alloy illustrated in (a) is less susceptible to LBZ's than the lower hardenability Fe-0.1C-1Si wt.% alloy shown in (b) [26].

Fracture Toughness

Much of the literature about mechanical toughness tends to focus on micromechanisms, test methodology or procedures for using experimental data in designing for structural integrity. By contrast, there is very little work on predicting the fracture toughness given a complex set of variables. This difficulty is illustrated by considering some basic concepts of fracture mechanics. The critical value K_{IC} of the stress intensity which must be exceeded to induce rapid crack propagation is the product of two terms:

$$K_{IC} = \text{stress} \times \text{distance}^{\frac{1}{2}} \tag{2}$$

where the stress is a fracture stress σ_F which can be measured independently using notched tensile specimens. It can be related to the microstructure via (for detailed references see [3]):

$$\sigma_F \propto \left[\frac{E\gamma_p}{\pi(1-\nu^2)c}\right]^{\frac{1}{2}} \tag{3}$$

where E is the Young's modulus and ν is the Poisson's ratio. γ_p is the effective work done in creating a unit area of crack plane, estimated to be about $14\,\mathrm{J\,m^{-2}}$ for many iron–base microstructures; it is much larger than a surface energy (typically $1\,\mathrm{J\,m^{-2}}$) because of the plastic zone which moves with the crack tip. This value of $14\,\mathrm{J\,m^{-2}}$ seems to apply to a wide variety of steel microstructures, which is surprising given that they often have quite different deformation characteristics. In any event, there is no obvious way of relating γ_p to details of the microstructure. The dimension c is the size of a sharp crack created by the fracture of a brittle microstructural constituent such as a cementite particle in wrought steels, or a non–metallic inclusion in a weld deposit.

The other parameter in equation 3, distance$^{\frac{1}{2}}$, refers to a distance ahead of the crack tip, within which the stress is large enough to cause the fracture of brittle crack–initiators. It is well–defined for coarse microstructures but not for many useful microstructures.

The temperature dependence of the fracture toughness of steels seems to be very well–behaved. Wallin [3] has shown that the shape of the toughness versus temperature curve is essentially the same for all structural steels, making it possible to define a universal dependence as follows:

$$\Delta K = 77 \exp\{0.019(T - T_0)\} \qquad \mathrm{MPa\,m^{1/2}} \qquad (4)$$

where ΔK is a change in toughness due to a corresponding change in temperature T. T_0 is a "transition temperature" where the fracture toughness for a 25 mm thick specimen is 100 $\mathrm{MPa\,m^{1/2}}$. This equation ought to apply to weld metals although T_0 would have to be determined experimentally.

There are, therefore, well–defined concepts of fracture mechanics, relating stress and crack–dimensions. These relationships cannot be used predictively because in each application they rely on experimental data generated for the specific material investigated. There is only a qualitative understanding of the factors that control toughness.

Neural Networks

All is not lost. There is a very promising method [27–30] for creating quantitative models for mechanical properties, as follows.

The usual approach when dealing with difficult problems is to correlate the results against chosen variables using linear regression analysis; a more powerful method of empirical analysis involves the use of neural networks. Since the method has been described elsewhere [27–30], what follows is a mere introduction.

In conventional regression analysis the data are best–fitted to a specified relationship which is usually linear. The result is an equation in which each of the inputs x_j is multiplied by a weight w_j; the sum of all such products and a constant θ then gives an estimate of the output $y = \sum_j w_j x_j + \theta$. Relationships like these are used widely in the welding industry, for example, in the formulation of the famous *carbon equivalents*:

$$\mathrm{IIW} \quad > 0.18\,\mathrm{wt.\%\ C}$$

$$\mathrm{CE} = \mathrm{C} + \frac{\mathrm{Mn} + \mathrm{Si}}{6} + \frac{\mathrm{Ni} + \mathrm{Cu}}{15} + \frac{\mathrm{Cr} + \mathrm{Mo} + \mathrm{V}}{5} \qquad \mathrm{wt.\%}$$

or in the expression of mechanical properties as a function of the chemical composition (after Glynn Evans):

$$\text{yield strength / MPa} = 484 + 57 \times w_{Cu}$$

where w_{Cu} is the weight percent of copper in as–welded "carbon–manganese" manual metal arc welds. It is well understood that there is risk in using the relationships beyond the range of fitted data, but the risk is not quantified.

With neural networks, the input data x_j are again multiplied by weights, but the sum of all these products forms the argument of a hyperbolic tangent. The output y is therefore a non–linear function of x_j, the function usually chosen being the hyperbolic tangent because of its flexibility. The exact shape of the hyperbolic tangent can be varied by altering the weights (Fig. 8a). Further degrees of non–linearity can be introduced by combining several of these hyperbolic tangents (Fig. 8b), so that the neural network method is able to capture almost arbitrarily non–linear relationships.

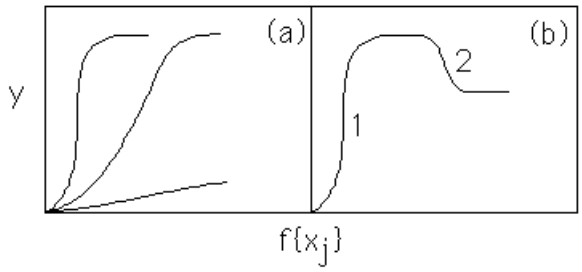

Fig. 8: (a) Three different hyperbolic tangent functions; the "strength" of each depends on the weights. (b) A combination of two hyperbolic tangents to produce a more complex model.

Fig. 9 illustrates the complexity of the surface that can be produced when representing the output (vertical axis) as a function of two inputs using just four hyperbolic tangents. A potential difficulty with the ability to produce complex, non–linear functions is the possibility of overfitting of data. It is possible, for example, to produce a neural network model for a random set of data. To avoid this difficulty, the experimental data can be divided into two sets, a *training* dataset and a *test* dataset. The model is produced using only the training data. The test data are then used to check that the model generalises when presented with previously unseen data. Other facilities

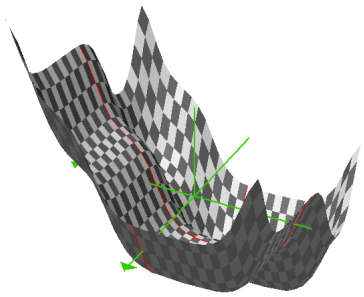

Fig. 9: Variation in the output (vertical axis) as a function of two input variables, the surface being represented with just four hyperbolic tangent functions.

are introduced in the section dealing with Bayesian inference [27,28].

It is common practice in regression analysis to best fit a function to the data, *i.e.* to use the most probable values of the weights for a given model. This results in an overall error obtained by comparing the predictions against experimental values, with no indication of the uncertainty as a function of position in the input space. MacKay has developed a treatment of neural networks in a Bayesian framework [27,28], which allows the calculation of error bars representing the uncertainty in the fitting parameters. The method recognises that there are many functions which can be fitted or extrapolated into uncertain regions of the input space, without unduly compromising the fit in adjacent regions which are rich in accurate data. Instead of calculating a unique set of weights, a probability distribution of sets of weights is used to define the fitting uncertainty. The error bars therefore become large when data are sparse or locally noisy. The Bayesian framework is also used to avoid overfitting and automatic relevance determination [27,28] We shall now proceed to explain the Bayesian method which has now become vital in the study of weld mechanical properties.

Bayesian Inference

It is worth introducing gaussians which are assumed in the inference procedures described below [27,28,31]. Given a continuous variable x, a gaussian probability distribution is

$$P\{x\} = \frac{1}{\sigma\sqrt{2\pi}} \exp\left\{-\frac{(x-\overline{x})^2}{2\sigma^2}\right\}$$

where σ is the standard deviation or the width of the gaussian, $\overline{x}$ is the mean and the term outside of the exponential normalises the distribution such that the area under the curve (*i.e.* total probability) is one.

Bayesian Inference: Given a set of experimental data in which the inputs and output are related by a straight line, our goal is to infer the fitting parameters as a probability distribution of weights rather than a single set of best–fit weights.

Prior Beliefs: Consider a straight line model in the absence of any data:

$$y\{x\} = w_1 x_1 + w_2 x_2 \tag{5}$$

where w_1 is the slope and w_2 the constant since we set $x_2 = 1$. The vector describing the set of weights $(w_1,\ w_2)$ is written $\mathbf{w}$. Vectors are identified in the text using bold font.

In the absence of data we have some *a priori* beliefs (Fig. 10) about the values of w_i, which are expressed as a (gaussian) probability distribution function

$$P(w_i) = \exp\{-\alpha w_i^2/2\}/Z$$

where Z is the normalising factor and $\alpha = 1/\sigma_w^2$ where σ_w is the standard deviation in the distribution of w_i.

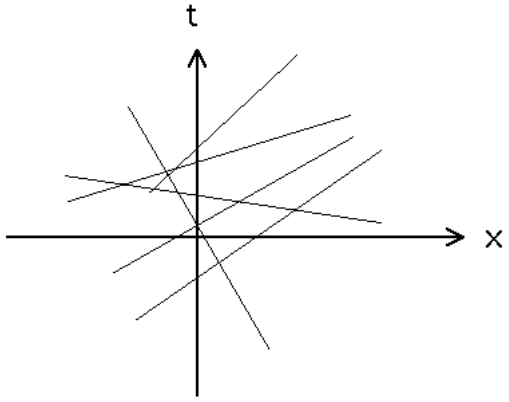

Fig. 10: Prior beliefs about straight line models

The Data: Suppose we now have some experimental data $D = \{\mathbf{x}_m, t_m\}$, where $m = 1 \ldots N$ is a label running over the pairs of inputs $\mathbf{x}_m$ and target t_m. The set of inputs and targets are written $\{x\}$ and $\{t\}$ respectively.

Given the data, a line with connections $\mathbf{w}$ can make predictions about the target output t_m as a function of the input vector $\mathbf{x}_m = (x_1, x_2)_m$ in accordance with the probability distribution

$$P(t_m|\mathbf{w}, \mathbf{x}_m) = \exp\left\{-\frac{\beta(t_m - y\{\mathbf{x}_m\})^2}{2}\right\} \Big/ Z'$$

with $\sigma_\nu^2 = 1/\beta$, where σ_ν is the perceived level of noise in the output (Fig. 11).

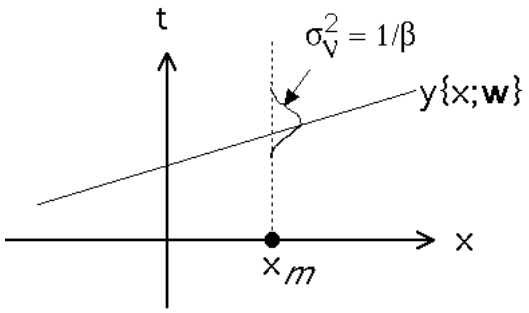

Fig. 11: Gaussian noise associated with the output.

Bayes' Rule: The desired probability distribution of weights is obtained from Bayes' rule as the *likelihood* × *prior*

$$P(\mathbf{w}|\{t\},\{x\}) \propto P(\{t\}|\mathbf{w},\{x\}) \times P(\mathbf{w})$$

$$P(\mathbf{w}|\{t\},\{x\}) = \frac{P(\{t\}|\mathbf{w},\{x\}) \times P(\mathbf{w})}{P(\{t\}|\{x\})}$$

$$= \frac{\exp\{-M\{\mathbf{x}\}\}}{Z_M}$$

where

$$M\{\mathbf{x}\} = \frac{\alpha}{2}\sum_i w_i^2 + \frac{\beta}{2}\sum_{m=1}^{N}\left(t_m - \sum_i w_i x_{m,i}\right)^2$$

A probability distribution of weights is illustrated in Fig. 12a. This distribution can be used to derive the error bars as shown in Fig. 12b.

Charpy Toughness

We can now see how these concepts can be applied to one of the most common tests used to characterise the energy absorbed during fracture, the Charpy test. A square section notched bar is fractured under specified conditions and the energy absorbed during fracture is taken as a measure of toughness. The Charpy test is empirical in that the data cannot be used directly in engineering design. It does not provide the most searching mechanical conditions. The sample has a notch, but this is less than the atomically sharp brittle crack. Although the test involves impact loading, there is a requirement to start a brittle crack from rest at the tip of the notch, suggesting that the test is optimistic in its comparison against a propagating brittle crack [32]. Most materials can be assumed to contain sub–critical defects so that the initiation of a crack seems seldom to be an issue.

The Charpy test is nevertheless a vital quality control measure which is specified widely in international standards, and in the ranking of samples in research and development exercises. It is the most common first assessment of toughness and in this sense

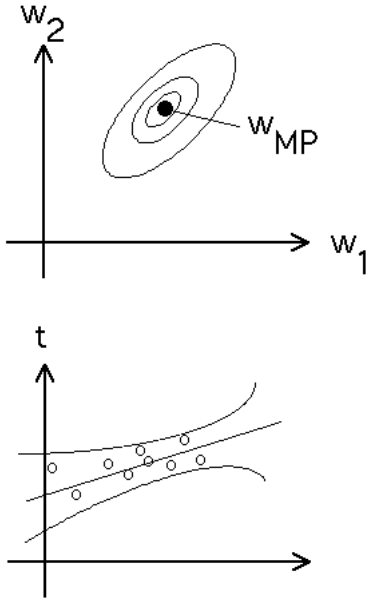

Fig. 12: (a) Contours showing the probability distribution of weights. w_{MP} represents the most probable set. (b) Plot showing the error bounds about the most probable line.

has a proven record of reliability. The test is usually carried out at a variety of temperatures in order to characterise the ductile–brittle transition intrinsic to body–centred cubic metals with their large Peierls barriers to dislocation motion.

The toughness of a steel depends on many variables; that of a weld is dependent on many more. It is not possible to predict the Charpy toughness of a weld with any reliability.

Some of the variables that influence the impact toughness of a ferritic steel weld are listed in Table 1.

A common belief is that the toughness of ferritic steel welds and of ferritic steels in general can be improved by adding nickel as an alloying element. The mechanism for this in not understood but it is speculated that those solutes which enable the cross–slip of screw dislocations, by reducing their dissociation, make them less effective as crack nuclei [33].

However, attempts at improving the Charpy toughness of commercial welding alloys of the type used in the fabrication of submarines, by increasing the nickel concentration, have consistently failed. These alloys have a base chemical composition which is summarised as follows:

Fe–0.03C–0.5Si–2Mn–0.5Cr–0.5Mo–3Ni wt%

A part of the reason for the failure to improve toughness using nickel is that we tend to generalise

Yield strength	Ultimate tensile strength
carbon	silicon
manganese	chromium
nickel	tungsten
sulphur	phosphorus
titanium	aluminium
nitrogen, hydrogen	oxygen *etc.*
primary microstructure	secondary microstructure
α, α_W, α_b, α_a *etc.*	welding parameters
degassing	heat treatment

Table 1: Some variables controlling Charpy toughness.

observations made on a limited range of alloy chemistry. A neural network model was therefore created to cover a very large range of welding alloys; its purpose was to estimate the Charpy toughness as a function of many of the variables indicated in Table 1. Calculations using this model showed that in the class of welds described above, nickel is only effective in improving the Charpy toughness when the concentration of manganese is small (Fig. 13) [34]. No experiments were done in creating the model, which relied on published data. The only experiments were those conducted after the modelling, involving the manufacture of a new welding alloy which verified the results shown in Fig. 13.

Naturally, the plot (Fig. 13) does not in itself explain the mechanism by which the toughness is enhanced by nickel at low manganese concentrations, and *vice versa*. But it does suggest some clear paths for investigation. The fact that even at low manganese levels, nickel reduces toughness beyond a concentration of about 7 wt% points towards solidification–induced chemical segregation as the culprit. This has now been proven [35], that segregation leads to hard zones in the weld, and that segregation is prominent at high manganese concentrations (and high Ni when the Mn concentration is low).

Conclusions & Recommendation

Physical models for complex properties are very far from being able to be used for quantitative predictions.

Models based on an examination of a limited dataset lead to relationships which do not generalise. Indeed, it is difficult to understand why such models are created given the vast quantities of experimental data which are openly available. It is not surprising that such models are susceptible to abuse.

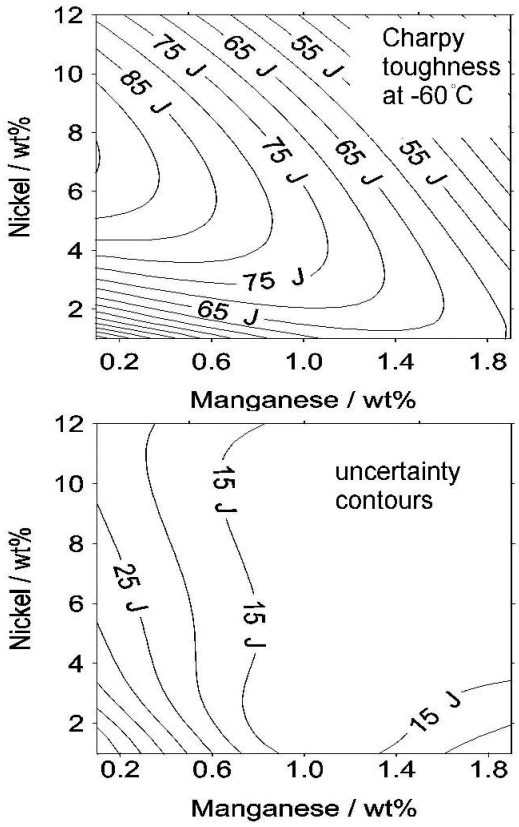

Fig. 13: The combined effect of manganese and nickel on the calculated toughness for -60°C, of weld metal produced using arc welding with a heat input of 0.8 kJ mm^{-1}, with a base composition (wt%) 0.025 C, 0.37 Si, 0.006 S, 0.013 P, 0.21 Cr, 0.4 Mo, 0.011 V, 0.03 Cu, 0.039 O, 0.008 Ti, 0.019 N, and an interpass temperature of 250°C. (a) Contours showing the Charpy toughness. (b) Contours showing the $\pm 1\sigma$ uncertainty in the calculations.

Recommendation: the best way to model mechanical properties is by using neural networks within a Bayesian framework. The models have greater generality, they deal neatly with scatter and provide a framework for identifying complex patterns which are otherwise difficult to perceive. Future effort should be focused on this technique and in the compilation of existing data.

Acknowledgments: I am deeply grateful to David MacKay for his help with Bayesian inference and to Thomas Sourmail and Marimuthu Murugananth for helpful discussions.

References

1. T. Zacharia, J. M. Vitek, J. A. Goldak, T. A. Debroy, M. Rappaz and H. K. D. H. Bhadeshia: *Modelling and Simulation in Materials Science and Engineering* 3, 265–288 (1995)
2. H. K. D. H. Bhadeshia: *Mathematical Modelling of Weld Phenomena III,* eds H. Cerjak and H. Bhadeshia, Institute of Materials, London 229–284 (1997)
3. H. K. D. H. Bhadeshia: *Second Griffith Conference on Micromechanisms of Fracture and Their Structural Significance,* Institute of Materials, London, 15–24 (1995)
4. H. Tamehiro, T. Takeda, S. Matsuda, K. Yamamoto and N. Okumura: *Trans. ISIJ* 25, 982–988 (1985)
5. A. J. R. Loureiro and A. A. Fernandes: *Welding Journal Research Supplement* 73, 225s–232s (1994)
6. J. C. Ion, K. E. Easterling and M. F. Ashby: *Acta Metall.* 32, 1949–1962 (1984)
7. E. A. Metzbower, H. K. D. H. Bhadeshia and R. H. Philips: *Materials Science and Technology* 10, 56–59 (1994)
8. H.K.D.H. Bhadeshia, L.–E. Svensson & B. Gretoft: *Acta Metall.* 33, 1271–1283 (1985)
9. H. K. D. H. Bhadeshia and L.–E. Svensson: *Mathematical Modelling of Weld Phenomena,* eds H. Cerjak and K. Easterling, Institute of Materials, London 109–182 (1993)
10. S. S. Babu, S. A. David, J. M. Vitek, K. Mundra and T. DebRoy: *Materials Science and Technology* 11, 186–199 (1995)
11. H. K. D. H. Bhadeshia and D. V. Edmonds: *Metal Science* 17, 411–419 (1983)
12. Y. Tomota, K. Kuroki, T. Mori and I. Tamura: *Materials Science and Engineering* 24, 85–94 (1976)
13. H. K. D. H. Bhadeshia and D. V. Edmonds: *Metal Science* 14, 41–49 (1980)
14. C. H. Young and H. K. D. H. Bhadeshia: *Materials Science and Technology* 10, 209–214 (1994)
15. Y. Tomita and K. Okabayashi: *Metall. Trans.* 14A, 485–492 (1983)
16. D. Venugopalan and J. S. Kirkaldy: *Hardenability concepts with applications to steels,* eds D. V. Doane and J. S. Kirkaldy, TMS–AIME, Warrendale, USA 249–268 (1977)
17. J. D. Robson and H. K. D. H. Bhadeshia: *Materials Science and Technology* 13, 631–644 (1997)
18. C. Downs and H. K. D. H. Bhadeshia: *Unpublished work* (2001)
19. T. Cool and H. K. D. H. Bhadeshia: *Science and Technology of Welding and Joining* 2, 36–42 (1997)
20. F. H. Lange: *Correlation Techniques,* Iliffe Books Ltd., London, U. K. 76–77 (1967)
21. S. Karlin and H. M. Taylor: *A First Course in Stochastic Processes,* Academic Press, New York, U. S. A., 495–502 (1975)
22. A. A. B. Sugden and H. K. D. H. Bhadeshia: *Recent Trends in Welding Science and Technology,* eds. S. A. David and J. M. Vitek, ASM International, Ohio, U. S. A., 745–748 (1989)
23. D. Fairchild: *Private communication to H. K. D. H. Bhadeshia* (1995)
24. J. Y. Koo and A. Ozekcin : *Welding Metallurgy of Structural Steels,*ed J. Y. Koo, TMS–AIME, Warrendale, PA, USA 119–136 (1987)
25. S. Aihara and K. Okamoto: *Metallurgy, Welding and Qualification of Microalloyed Steel Weldments,* eds J. T. Hickey *et al.*, AWS, Florida 402–427 (1990)
26. S. Suzuki, G. I. Rees and H. K. D. H. Bhadeshia: *Modelling and Control of Joining Processes,* ed. T. Zacharia, AWS, Florida, U.S.A. 186–194 (1993)
27. D. J. C. MacKay: *Neural Computation,* 4, 415–447 (1992)
28. D. J. C. MacKay: *Neural Computation,* 4, 448–472 (1992)
29. H. K. D. H. Bhadeshia: *ISIJ International* 39, 966–979 (1999)
30. D. Cole, C. Martin-Moran, A. Sheard, H. K. D. H. Bhadeshia and D. J. C. MacKay: *Science and Technology of Welding and Joining* 5, 81–89 (2000)
31. P. M. Lee: *Bayesian Statistics,* Edward Arnold, London 1989 ()
32. A. H. Cottrell: *European Review* 1, 169–176 (1993)
33. W. C. Leslie: *Physical Metallurgy of Steels* McGraw–Hill International Book Company, London, 1982 ()
    124
34. M. Murugananth, H. K. D. H. Bhadeshia, E. Keehan, H. O. Andren, L. Karlsson: *Mathematical Modelling of Weld Phenomena VI,* eds H. Cerjak and H. Bhadeshia, Institute of Materials, London in press (2002)
35. M. Murugananth: *Unpublished work* (2002)